Materials Science in Semiconductor Processing 39 (2015) 79–83

Contents lists available at ScienceDirect

Materials Science in Semiconductor Processing

journal homepage: www.elsevier.com/locate/mssp

Short Communication

An Na source via MoNa intermediate layer for three-stage evaporation of Cu(in, Ga)Se_2 solar cells

Huan-Hsin Sung [a], Du-Cheng Tsai [a], Zue-Chin Chang [b], Shih-Chang Liang [c], Fuh-Sheng Shieu [a,*]

[a] Department of Materials Science and Engineering, National Chung Hsing University, Taichung 40227, Taiwan, ROC
[b] Department of Mechanical Engineering, National Chin-Yi University of Technology, Taichung 41170, Taiwan, ROC
[c] Material and Electron-Optics Research Division, Chung-Shan Institute of Science and Technology, Long Tan 32552, Taiwan, ROC

ARTICLE INFO

Available online 15 May 2015

Keywords:
SIMS
CIGS solar cell
MoNa thin film

ABSTRACT

In this study, an Na source was integrated into the back contact stack, which is a MoNa layer. MoNa layers with varying thicknesses were deposited on Al_2O_3 substrate as intermediate layers of an Mo back contact by DC magnetron sputtering of a Mo-10 at% Na target. We examined the effect of MoNa thickness on the standard production of Cu(In, Ga)Se_2 (CIGS) solar cell fabricated using three-stage evaporation. The structure of the MoNa layer was composed of fibers with considerably small grain size (~5 nm). By contrast, the Mo layer presented a columnar structure with relatively large grain size. The Na concentration in the CIGS absorber can be adjusted by varying the thickness of the MoNa layer. Cell efficiency was heavily raised from 2.08% to 11.7% using MoNa layer as Na source. However, the enhanced deliquescence property with MoNa thickness limited further improvement in cell efficiency.

1. Introduction

Cu(In, Ga)Se_2 (CIGS) is an attractive candidate for thin film photovoltaic devices because it is a direct-gap semiconductor with an appropriate band gap of approximately 1 eV and possesses one of the highest known absorption coefficients (10^5 cm^{-1}) for solar radiation for any semiconductor. Jackson et al. claimed a new world record of 21.7% efficiency for CIGS solar cells on soda-lime glass (SLG) by three stage co-evaporation [1]. Na incorporated into CIGS absorber layers are significantly beneficial in enhancing cell efficiencies. The influence of Na has been studied to some extent in the CIGS community; however, the exact mechanism behind the improvement in efficiency remains unknown. Main Na studies point toward the following conclusions. Na catalyzes the oxidation of Se vacancies in the grain boundaries, leading to passivation of the positively charged traps [2,3]. Ga and In are replaced by Na to $Na_{In;Ga}$, which then acts as a shallow acceptor, resulting in increased hole concentration and corresponding improved p-type CIGS character [4–6]. The compensating donor defect In_{Cu} is eliminated when Cu is replaced by Na [7]. Na also influences CIGS growth, such as Ga/In interdiffusion behavior, preferred orientation, and grain sizes [8–10].

The usual form of Na incorporation is diffusion from a SLG through the Mo back contact during CIGS deposition. However, these methods require high temperature annealing to diffuse Na into the CIGS absorber, thereby limiting the development of fabricated solar cells on Na-free substrates, such as stainless steel or polymer film.

The exact amount of Na incorporation from the SLG is not well designed and controlled. To solve these problems, numerous research groups have tried to supply Na from

* Corresponding author. Tel.: +886 4 2284 0500; fax: +886 4 2285 7017.
E-mail address: fsshieu@dragon.nchu.edu.tw (F.-S. Shieu).

http://dx.doi.org/10.1016/j.mssp.2015.04.037
1369-8001/

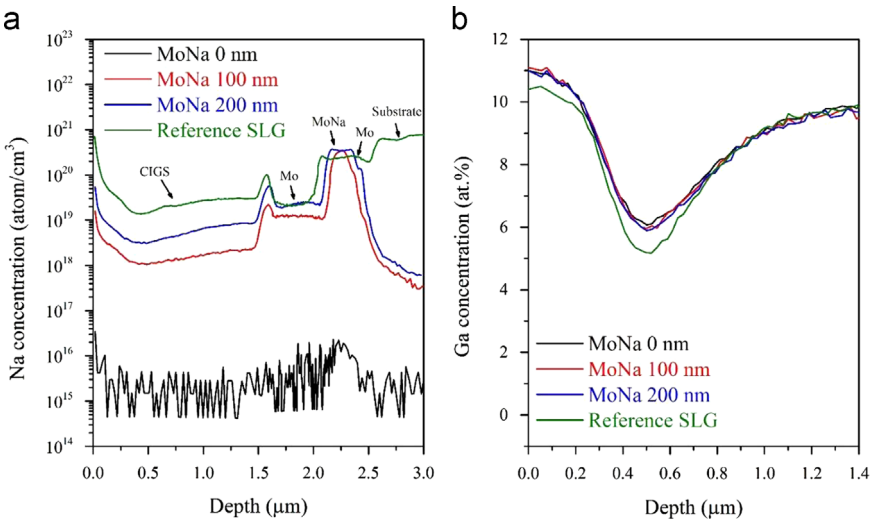

Fig. 1. SIMS depth profiles of elemental (a) Na and (b) Ga distribution for Mo/MoNa/Mo/CIGS stacked layer with different thicknesses of MoNa layer on Al_2O_3 substrates and reference SLG.

external sources, such as NaF and Na_2S [11–13]. However, this approach has presented a problem of adhesion between CIGS and Mo. Another problem is the residual F elements, which may occur when CIGS films are deposited on NaF, especially at lower deposition temperature. These factors are responsible for cell performance, and thus, need to be improved. Another source of usable Na would be an Na-containing Mo layer instead of a pure Mo layer, which eliminates the need to extract Na control and suitable for Na-free substrates [14]. However, the present results are not fully conclusive. The interface structure of the Na-doped Mo layer remains unclear.

In this study, we prepared Mo/MoNa/Mo multilayer structure on Al_2O_3 substrate to serve as cell back contact. This study aimed to find a suitable concentration of Na in CIGS absorber layer by adjusting the thickness of the MoNa layer. Comparison sample was also prepared on the laboratory-standard SLG substrate with a bilayer Mo back contact. The interface structure of the MoNa layer and the performance of CIGS solar cell were studied.

2. Experimental

The Na-free substrates used in this study were polished ceramic Al_2O_3 substrates. The SLG substrate without MoNa layer was used for reference. The back contact consisted of a sandwich stack structure Mo/MoNa/Mo layer. A compound target of Mo and Na_2MoO_4 was used for deposition of the MoNa layer. Na accounted for a total of 10% in atomic percentage.

The 100 nm-thick Mo was deposited on the substrate using a discharge current of 0.8 A and a working pressure of 10 mTorr (The thickness of the first Mo layer for reference SLG is 500 nm.) A MoNa layer with thickness varying from 0 to 200 nm was subsequently deposited under a discharge current of 0.8 A and a working pressure of 7.5 mTorr. Finally, the 500 nm-thick Mo was deposited on top of the MoNa layer at a discharge current of 0.8 A and a working pressure of 5 mTorr.

The quaternary CIGS absorber layer was deposited using the typical 3-stage process. In the first stage, In, Ga, and Se were co-evaporated at 350 °C substrate temperature to form an $(In, Ga)_2Se_3$ layer. In the second stage, the substrate temperature was increased to 550 °C, and then Cu and Se were co-evaporated until a Cu-rich film was formed. In the third stage, In, Ga, and Se were co-evaporated at 550 °C to obtain a Cu-poor CIGS absorber layer. The Cu/(In+Ga) and Ga/(In+Ga) composition ratios of the CIGS films were approximately 0.86 and 0.31, respectively, as determined by an X-ray fluorescent spectrometer (XRF, Solar Metrology SMX-BEN). Solar cells with substrate/Mo/MoNa/Mo/CIGS/CdS/i-ZnO/ZnO:Al/Ni/Al/Ni structure were completed. The CdS buffer layer was prepared by chemical bath deposition (CBD) using $CdSO_4$ as Cd salt, thiourea as sulfur precursor, and NH_3 as complexing agent. The undoped i-ZnO and ZnO:Al window layer and Ni/Al/Ni grids were deposited through RF magnetron sputtering.

Crystal structures were analyzed with an X-ray diffractometer (XRD, MacScience MXP3) using Cu Kα radiation at a scanning speed of 2°/min. The scanning range was 20–80°. Morphological studies were carried out using a field emission scanning electron microscope (FESEM, JEOL JSM-6700F) system. Microstructural examination was performed using a high-resolution transmission electron microscope (HRTEM, JEM-2100F). Composition depth profile was analyzed using a secondary ion mass spectroscopy (SIMS, CAMECA IMS-7f) system. Conversion efficiency was measured using a reference solar cell under AM 1.5 and 100 mW/cm^2 conditions after correction.

3. Results and discussion

Fig. 1a shows the SIMS depth profile of the Na element in the Mo/MoNa/Mo/CIGS stacked layer with different thicknesses of MoNa layer on the Al_2O_3 and reference SLG. Na solubility in CIGS single crystals is very low (only about 0.1 at%), such that Na resides at grain boundaries,

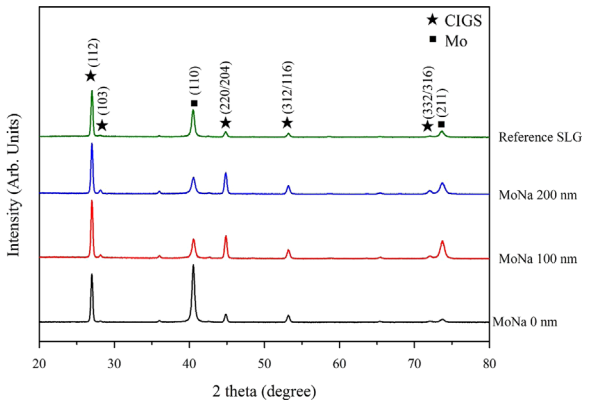

Fig. 2. XRD pattern of Mo/MoNa/Mo/CIGS stacked layer with different thicknesses of MoNa layer on Al_2O_3 substrates and reference SLG.

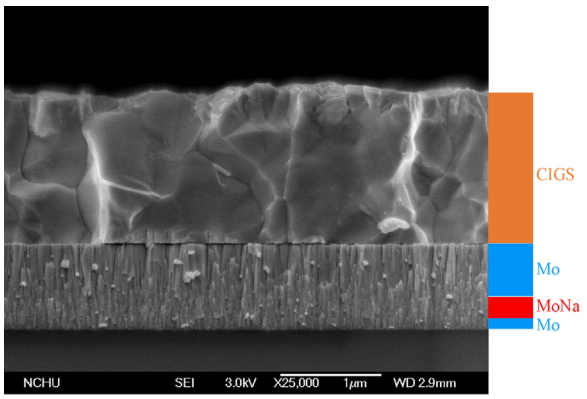

Fig. 3. SEM image of Mo/MoNa/Mo/CIGS stacked layer with 200 nm-thick MoNa layer on Al_2O_3 substrates.

interface, and surface when Na continuously diffuses through the Mo layer from the SLG substrate or MoNa layer during the CIGS grain growth. Higher Na concentration in the interface and surface regions indicates the accumulation of Na ions because a high defect density in the interface and surface regions is favorable for capturing Na ions. Moreover, the depth profile of Na presents a parabolic change in CIGS absorber layer. This behavior is attributed to the fact that the Na diffusion is already in progress during the deposition of the $(In, Ga)_2Se_3$ precursor film, and that Na begins to spread out upward and downward in the beginning of the CIGS grain growth. The amount of Na incorporated into CIGS depends on the thicknesses of the MoNa layer, and the Na concentration in the CIGS layer increases with increasing MoNa thickness, namely, with increasing Na sources. Compared with the reference SLG, which shows a relatively high concentration of Na, it is also found to have similar depth profiles using an Al_2O_3 substrate with a precursor MoNa layer, proving that the MoNa layer is a viable Na source material for this kind of experiments.

Meanwhile, the depth profile of Ga in CIGS layer is detected (Fig. 1b). The CIGS absorber layers exhibit a parabolic Ga profile across the layer, which is attributed to the absence of the Ga source during the second stage of the CIGS growth process, as well as the low diffusion coefficient of Ga in CIGS. Noticeably, the reference SLG shows a lower Ga concentration near the surface of CIGS layer and a steeper Ga concentration gradient than Al_2O_3 with MoNa, possibly because of the decreased concentration of metal vacancies eliminated by Na. In general, Na resides at the surface and grain boundary of CIGS, and act as a diffusion barrier for constitution atoms. However, no significant change was observed for Al_2O_3 with different MoNa thicknesses, indicating that the Na concentration was insufficiently high to impede Ga diffusion.

Fig. 2 shows the XRD patterns of the Mo/MoNa/Mo/CIGS stacked layer with different thicknesses of MoNa layer on the Al_2O_3 and reference SLG. The diffraction peaks corresponding to the (112), (103), (220)/(204), (312)/(116), and (332)/(316) lattice planes of a chalcopyrite CIGS phase, as well as to (110) and (211) of a body-centered cubic (bcc) Mo phase, were observed. With the increase in MoNa thickness, the intensity of the (110) peak significantly decreased, implying reduced crystallinity. These results may be attributed to the poorer crystallinity of MoNa layer.

Fig. 3 shows the SEM image of the Mo/MoNa/Mo/CIGS stacked layer with 200 nm-thick MoNa layer on the Al_2O_3 substrates. The Mo/MoNa/Mo layer reveals typical columnar structures, whereas the CIGS layer is characterized by large equiaxed grain structure. Fig. 4 shows the TEM micrographs with selected area diffraction (SAD) patterns of the Mo/MoNa/Mo/CIGS stacked layer with 200 nm-thick MoNa layer on the Al_2O_3 substrates. The layer-stacked structure of the Al_2O_3 substrate, the 100 nm-thick Mo layer, the 200 nm-thick MoNa layer, 500 nm-thick Mo layer, and 1.5 μm-thick CIGS layer were clearly observed (Fig. 4a). Three SAD patterns with equal size were labeled as Zones A, B, and C, and presented in Fig. 4b–d. Zone A shows a bcc pattern of rings, implying a smaller grain structure. Zone B contains arc-like bcc diffraction rings, indicating a larger grain size with obviously preferred orientation. Zone C reveals a large single-grain SAD with a chalcopyrite phase. Fig. 4e and f shows a higher magnification bright field image and a dark field image, respectively. The Mo layer has a typical columnar structure, while the MoNa layer exhibits fiber structures with very small grain size. The column width of the bottom and top Mo layers are approximately 23 nm and 12 nm, respectively. The MoNa layer has a considerably small fiber width of ~5 nm, indicating that Na impedes the grain growth of the MoNa layer.

Fig. 5 shows the *J–V* characteristics of CIGS solar cells prepared with different thicknesses of MoNa layer on the Al_2O_3 and reference SLG. The reference SLG displays a high efficiency of 13.16%. As expected, the Na-free sample without any Na source produced the lowest efficiency of all at 2.08%. Using the 100 nm-thick MoNa layer, the efficiency heavily increased to 11.70%, benefiting from an increase of the V_{oc} by 110 mV and J_{sc} by 21.44 mA/cm^2 and an absolute increase of the FF by 34%. The increase in efficiency may be caused by improved transport problems and lower defect density because Na increases the carrier concentration by defect passivation.

No further improvement in efficiency was observed when the MoNa thickness was increased to 200 nm. The

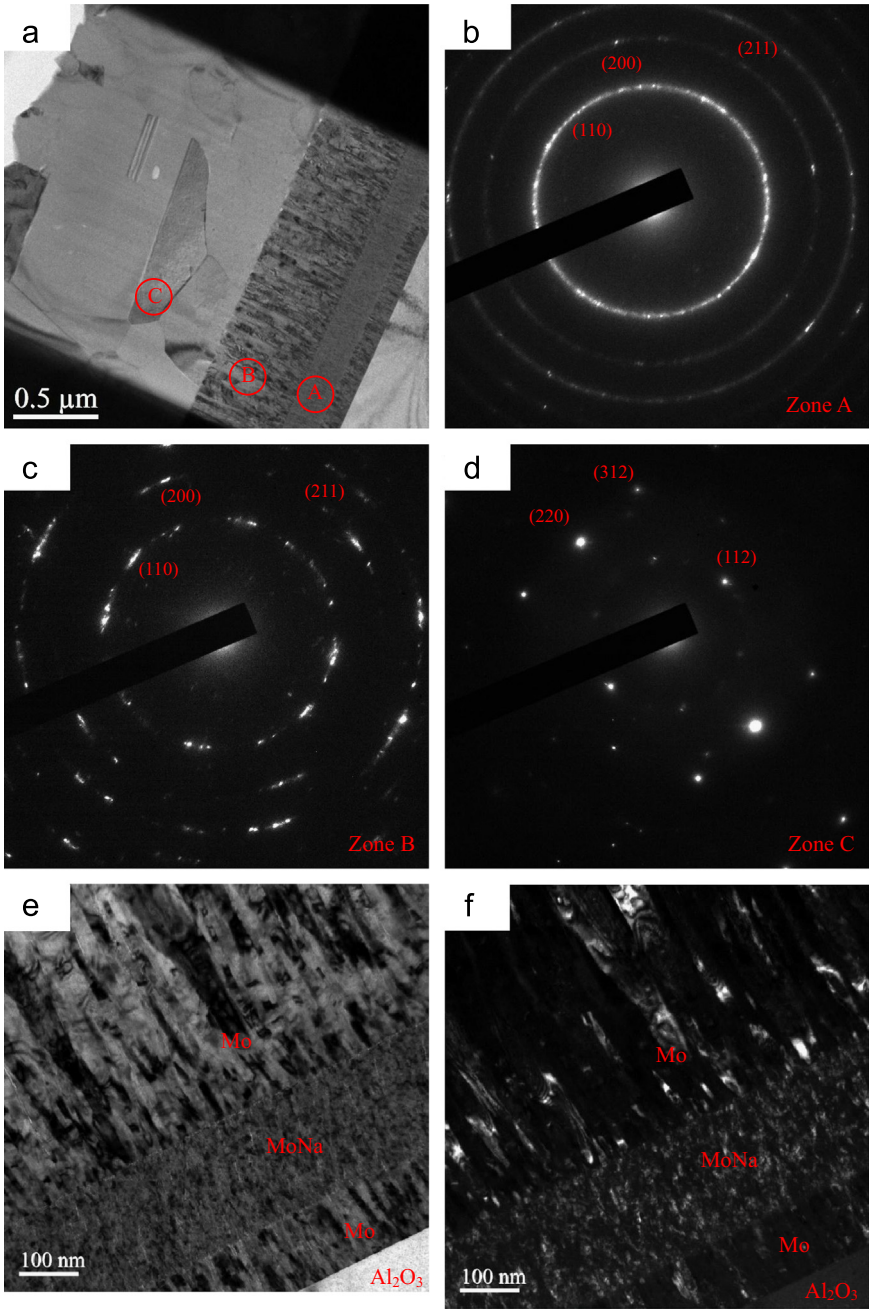

Fig. 4. Cross-sectional TEM micrographs with selected area diffraction (SAD) patterns of Mo/MoNa/Mo/CIGS stacked layer with 200 nm-thick MoNa layer on Al_2O_3 substrates. (a) Bright-field image. (b) SAD patterns of Zone A. (c) SAD patterns of Zone B. (d) SAD patterns of Zone C. (e) Higher magnification bright-field image. (f) Higher magnification dark-field image.

possible explanation is described as follows. Many of these Na compounds are very difficult to handle because of their unstable properties, such as deliquescence; thus, performance improvement of solar cells with satisfactory reproducibility has not been achieved. An intriguing finding is that the deliquescence phenomenon quickly occurs when Mo/MoNa/Mo film is exposed to air. The deliquescence accelerates with increasing MoNa thickness. This behavior can cause several negative effects, including the formation of second phase, increased electrical resistivity, and poorer adhesion, which deteriorates the performance of CIGS solar. In this study, a clear improvement in efficiency was observed when using the Mo/MoNa/Mo back contact, compared with using a Na-free Mo back contact. The MoNa layer is therefore responsible for the controlled release of Na that occurs as the CIGS absorber is formed. This study is a proof of concept that employing Mo-10 at% Na target to supplement Na by sputtering is an effective and feasible approach. However, the high deliquescence and chemical instability of the MoNa layer makes it

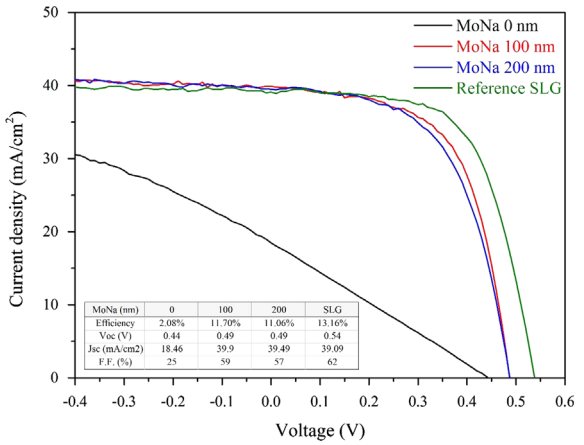

Fig. 5. *J–V* characteristics of CIGS solar cells prepared with different thicknesses of MoNa layer on Al_2O_3 substrates and reference SLG.

difficult to obtain a desired solar cell. Further research and development in the MoNa layer as Na source is still required.

4. Conclusion

This study employed Mo-10 at% Na target to prepare a MoNa layer on Al_2O_3 substrate as intermediate layers of an Mo back contact by DC magnetron sputtering. MoNa layers were used as Na source materials. The quantity of Na incorporated into the CIGS absorber layer through the Mo back contact layer was controlled by controlling the MoNa thickness. Compared with the Mo layer, the MoNa layer shows fiber structured grains with very small size and poor crystallinity. This observation leads to the interpretation that a significant amount of Na is already present at the grain boundaries after MoNa deposition, which impedes the grain growth of the MoNa layer. The extent of Na accumulation in the CIGS absorber layer depended strongly on the thickness of the MoNa layer, where an increase in the thickness of the MoNa layer showed enhanced Na out-diffusion performance. Completed solar cell utilizing MoNa was significantly higher than Na-free solar cell because of the increased carrier concentration by passivation of defects. However, high MoNa thickness limited the efficiency of the cell because of deliquescence property. Additional efforts are needed to solve the deliquescence problem of the thicker MoNa layers. Based on these data, MoNa may provide a manufacturing option for controllable Na incorporation in CIGS solar cells.

Acknowledgments

The authors gratefully acknowledge the financial support for this research by the Ministry of Science and Technology of Taiwan under Grant no. NSC103-2221-E-005-020-MY3. The present work was also supported in part by the Center for Micro/Nano Science and Technology of the National Cheng Kung University.

References

[1] P. Jackson, D. Hariskos, R. Wuerz, O. Kiowski, A. Bauer, T. M. Friedlmeier, M. Powalla, Phys. Status Solidi-Rapid Res. Lett. 7 (2015) 28–31.
[2] D.K. Schroder, Semiconductor Material and Device Characterization, third ed. Wiley, Hoboken, 2006.
[3] D.W. Niles, K. Ramanathan, F. Hasoon, R. Noufi, B.J. Tielsch, J.E. Fulghum, J. Vac. Sci. Technol. A 15 (1997) 3044–3049.
[4] M. Contreras, B. Egaas, P. Dippo, J. Webb, J. Granata, K. Ramanathan, S. Asher, A. Swartzlander, R. Noufi, On the role of Na and modifications to Cu (In,Ga)Se_2, absorber materials using thin-MF (M=Na, K, Cs) precursor layers, in: Proceedings of the 26th IEEE Photovoltaic Specialists Conference Record, Anaheim, New York, pp. 359–362 1997.
[5] S. Ishizuka, A. Yamada, M.M. Islam, H. Shibata, P. Fons, T. Sakurai, K. Akimoto, S. Niki, J. Appl. Phys. 106 (2009) 034908.
[6] M. Bodegård, K. Granath, L. Stolt, Thin Solid Films 361 (2000) 9–16.
[7] D. Rudmann, G. Bilger, M. Kaelin, F.-J. Haug, H. Zogg, A.N. Tiwari, Thin Solid Films 431 (2003) 37–40.
[8] D. Rudmann, A.F. da Cunha, M. Kaelin, F. Kurdesau, H. Zogg, A.N. Tiwari, G. Bilger, Efficiency enhancement of Cu(In,Ga)Se_2 solar cells due to post-deposition Na incorporation, Appl. Phys. Lett. 84 (2004) 1129–1131.
[9] R. Caballero, C.A. Kaufmann, T. Eisenbarth, M. Cancela, R. Hesse, T. Unold, A. Eicke, R. Klenk, H.W. Schock, Thin Solid Films 517 (2009) 2187–2190.
[10] Y.M. Shin, D.H. Shin, J.H. Kim, B.T. Ahn, Curr. Appl. Phys. 11 (2011) S59–S64.
[11] J.H. Yun, K.H. Kim, M.S. Kim, B.T. Ahn, S.J. Ahn, J.C. Lee, K.H. Yoon, Thin Solid Films 515 (2007) 5876–5879.
[12] D. Rudmann Ph.D., dissertation, Effects of sodium on growth and properties of Cu(In,Ga)Se_2 thin films and solar cells, Swiss Federal Inst. Technol., Zurich, Switzerland, 2004.
[13] D.J. Schroeder, A.A. Rockett, Electronic effects of sodium in epitaxial $CuIn_{1-x}Ga_xSe_2$, J. Appl. Phys. 82 (1997) 4982–4985.
[14] L. Stolt, J. Hedström, J. Kessler, M. Ruckh, K.O. Velthaus, H.W. Schock, ZnO/CdS/$CuInSe_2$ thin-film solar cells with improved performance, Appl. Phys. Lett. 62 (1993) 597–599.